Available online at www.sciencedirect.com
SciVerse ScienceDirect
Ceramics International 38 (2012) 4369–4372
CERAMICS INTERNATIONAL
www.elsevier.com/locate/ceramint

Short communication

# Development of master sintering curve for field-assisted sintering of $HfB_2$–20SiC

Ravi K. Enneti [a,*], Manish G. Bothara [b], Seong-Jin Park [c], Sundar V. Atre [b]

[a] Research and Development, Global Tungsten and Powders Corp., Towanda, PA, United States
[b] Oregon Nanoscience and Microtechnologies Institute, Oregon State University, Corvallis, OR, United States
[c] Division of Advanced Nuclear Engineering (DANE) and Department of Mechanical Engineering, Pohang University of Science & Technology (POSTECH), Pohang, Republic of Korea

Received 24 October 2011; received in revised form 3 January 2012; accepted 4 January 2012
Available online 12 January 2012

**Abstract**

Field assisted sintering (FAST) or spark plasma sintering (SPS) has emerged as a promising technology for densification of ultra high temperature ceramics like $HfB_2$–20SiC at relatively low temperatures and shorter times. In the present study the concepts of master sintering curve (MSC) was applied to model the densification behavior of $HfB_2$–20SiC during FAST process. An activation energy of 300 kJ/mol was estimated for field assisted sintering of $HfB_2$–20SiC. The densification curves at various heating rates merged for activation energy of 300 kJ/mol confirming the applicability of MSC concepts to FAST process. The developed master sintering curves can be used to design sintering cycles and predict the densification of $HfB_2$–20SiC during FAST process.


*Keywords:* Field assisted sintering; Spark plasma sintering; Maser sintering curve; $HfB_2$–20SiC; Activation energy

## 1. Introduction

Borides, carbides and nitrides of the group IVB and VB transition metals exhibit high melting temperature in excess of 3000 °C and are considered ultrahigh temperature ceramics (UHTCs). Among the UHTCs, $HfB_2$ is identified as a potential candidate system for high temperature aerospace applications due to its excellent combination of properties such as chemical stability, high electrical and thermal conductivities, and resistance to erosion and corrosion [1–3]. However, $HfB_2$ exhibits poor oxidation resistance at high temperatures. The oxidation resistance of $HfB_2$ is increased with the addition of 20–30 vol.% SiC [3–5]. The densification of $HfB_2$–SiC system like other UHTCs requires long sintering cycles at high temperatures and external pressure [6]. In recent years, field assisted sintering (FAST) has emerged as a potential technology for densifying $HfB_2$–SiC using faster sintering cycles at low temperatures. In FAST technique the material is densified under the influence of external pressure and pulsed DC current [7–12].

In the past few years, master sintering curve (MSC) concepts have been successfully applied to model the densification behavior of metals and ceramics [13–17]. The master sintering curves relates the densification parameter $\phi(\rho)$ to sintering time and temperature as per the following equation

$$\phi(\rho) = \Theta(t, T) = \int_0^t \frac{1}{T} \exp\left(\frac{-Q}{RT}\right) dt \quad (1)$$

where $\Theta(\rho)$ is defined as work of sintering, $Q$ is the apparent activation energy, $R$ is the gas constant, $t$ is the time and $T$ is the absolute temperature. For an appropriate value of $Q$ the densification parameter $\phi(\rho)$ becomes independent of heating rate. Most of the MSC curves reported in the literature were developed for materials sintered by conventional sintering process (slow heating rates and long isothermal holds at appropriate sintering temperature). Recently MSC curves were developed for plasma compaction process [18]. There are however, no research studies reported on ability of the MSC concepts to model the densification of $HfB_2$–20SiC during FAST process. The primary objective of the present research is to verify the

* Corresponding author. Tel.: +1 570 268 5252.
*E-mail address:* ravi.enneti@globaltungsten.com (R.K. Enneti).

0272-8842/$36.00 
doi:10.1016/j.ceramint.2012.01.008

applicability of MSC concepts for the FAST process which involves high heating rates and shorter sintering cycles. The developed MSC curves will assist in designing sintering cycles to achieved high densification of $HfB_2$–20SiC during FAST process.

## 2. Experimental details

Ball milled $HfB_2$ (−325 mesh Cerac, USA) and SiC powders (1 μm, H.C. Starck, USA) were used as the starting powders. The powders were loaded into a 40-mm graphite die coated with BN and lined with graphite foil. The samples were sintered using FAST technique (FCT System GmbH, Rauenstein, Germany). The temperature was measured by an optical pyrometer focused on the bottom of a bore hole in the graphite punch approximately 5 mm from the powder. A vacuum of 150 Pa was maintained for the entire heating cycle. A pulsed DC current of 15 ms on and 5 ms off with a single pulse was used for heating. Experiments were carried out at a pressure of 40 kN and heating rates of 50 K/min, 100 K/min and 150 K/min. The samples were held at the maximum sinter temperature of 2373 K for 8 min.

## 3. Results and discussion

The raw data (time (s), temperature (°C) and displacement (mm)) were obtained for each FAST sintering run. The following steps were used for developing MSC from the obtained raw data:

1. The displacement in mm is converted to sample height (using the initial height, $h_0$, measured before the experiment).
2. The sintered density (g/cm$^3$) is calculated using the height, weight of powder in the die and cross sectional dimensions of the die that are fixed.
3. The density in g/cm$^3$ is converted to relative density.
4. Densification parameter $\phi(\rho)$, is estimated such that it is 0 when relative density is ∼40% (green density of samples) and 1 when relative density is maximum (∼99%).
5. Parameter, $\theta$ is calculated for one assumed value of $Q$.
6. $\phi(\rho)$ vs ln($\theta$) is plotted for each heating rate and assumed value of $Q$.
7. The difference (variance) between the curves at different heating rates is quantified.
8. The steps 5–7 are repeated for different values of $Q$.
9. The variance is plotted as a function of $Q$.
10. The plot $\phi(\rho)$ vs ln($\theta$) for $Q$ with minimum variance gives the MSC.

The MSC curves developed based on the above mentioned procedure for FAST sintering of $HfB_2$–20SiC for various values of $Q$ is shown in Fig. 1. The variance in the curves at different heating rates was estimated from the onset of densification for each assumed value of $Q$. Fig. 2 shows the plot of variance in the curves for different assumed values of $Q$. The plot shows minimum variance for a $Q$ value of 300 kJ/mol. The plot in Fig. 1 shows the curves at different heating rates merged into one curve for a $Q$ value of 300 kJ/mol. The curve of $\phi(\rho)$ vs ln($\theta$) at $Q$ value of 300 kJ/mol is the MSC for FAST sintering of

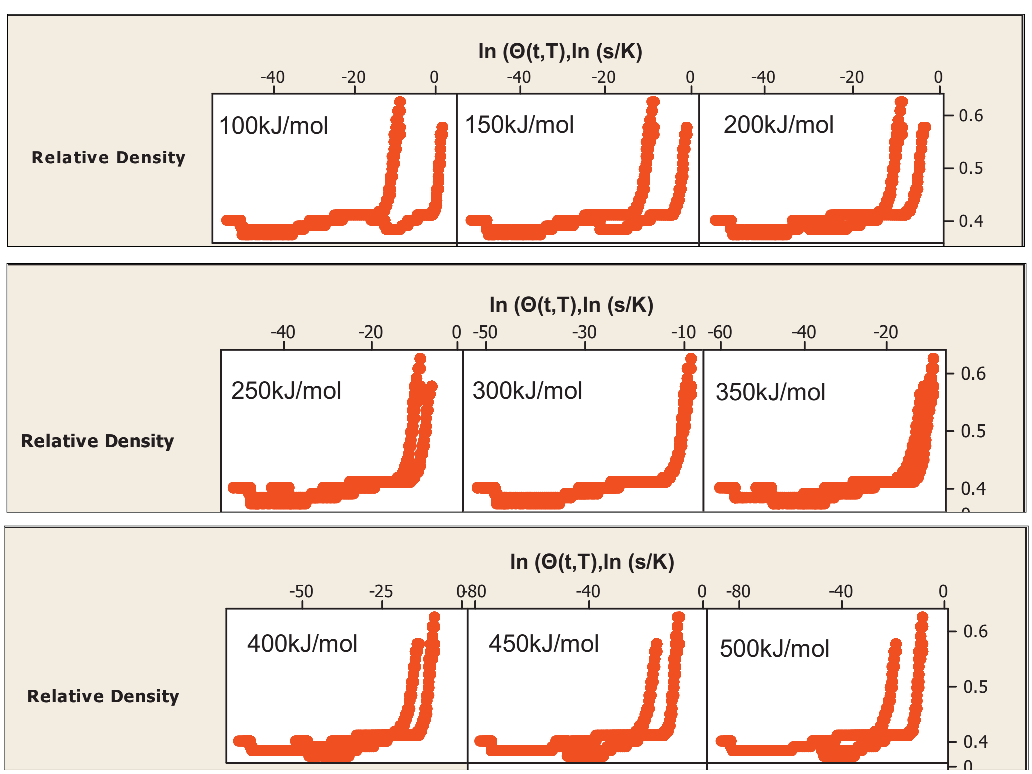


Fig. 1. MSC curves for FAST sintering of $HfB_2$–20SiC for various values of $Q$.

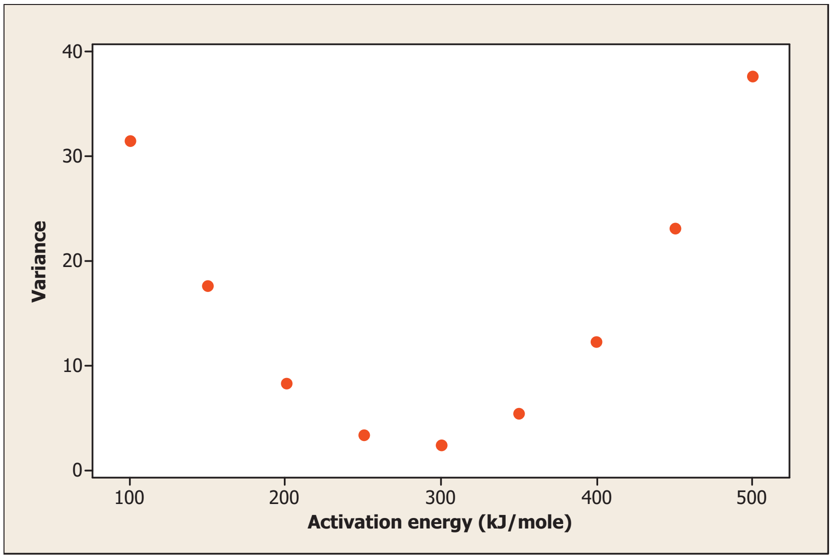


Fig. 2. Plot showing variance in curves at various heating rates for assumed values of $Q$.

Table 1
Comparison of the results obtained in the current study with prior studies focused on densification of $HfB_2$–20SiC. The volume % of SiC in Refs. [22,23] was 19 and 19.5% respectively.

| Technique | Additives | Process conditions | Sintered/relative density | Reference |
|---|---|---|---|---|
| HP | – | 2200 °C, 25 MPa, 1 h | ~100% | [19] |
| HP | – | 2000 °C, ~70 MPa, 2 h | 97% | [20] |
| HP | – | 1915 °C, 24 MPa | 100% | [21] |
| HP | 5.8 vol.% $Si_3N_4$ | 1850 °C, 30 MPa, ~2 h | 95.5% | [22] |
| HP | 3 vol.% HfN | 1900 °C, 50 MPa, ~4 h | >99.5% | [23] |
| SPS | – | 2100 °C, 40 kN, 50 °C/min, 0.13 h | 99.2% | Present study |
| SPS | – | 2100 °C, 40 kN, 150 °C/min, 0.13 h | 96.8% | Present study |

$HfB_2$–20SiC. The analysis thus confirms the applicability of MSC concepts to model the densification of $HfB_2$–20SiC during FAST process.

Table 1 shows the comparison of the results obtained in the present study with prior studies focused on densification of $HfB_2$–20SiC. The data in Table 1 confirms the advantages of using SPS technique to densify $HfB_2$–20SiC compared to hot pressing. The hot pressing technique requires significantly higher temperature, longer thermal cycles and higher pressures to obtain good densification in $HfB_2$–20SiC compared to SPS technique. The results also show that higher sinter densities can be obtained by SPS techniques without the addition of sintering aids.

## 4. Conclusion

A method was developed to construct MSC for materials sintered by FAST process. The applicability of MSC concepts to model the densification during sintering of $HfB_2$–20SiC by FAST process was confirmed. The MSC analysis estimated activation energy of 300 kJ/mol for sintering for of $HfB_2$–20SiC by FAST process.

## Acknowledgements

This work was partly supported by a summer fellowship from the American Society of Engineering Education. The authors further thank Carmen Carney and the Air Force Research Laboratory at the Wright-Patterson Air Force Base, OH for valuable assistance with the SPS experiments. The authors would like to thank financial and technical supports from the WCU (World Class University) program through the National Research Foundation of Korea funded by the Ministry of Education, Science and Technology (R31-30005).

## References

[1] F. Monteverde, Ultra-high temperature $HfB_2$–SiC ceramics consolidated by hot-pressing and spark plasma sintering, J. Alloys Compd. 428 (2007) 197–205.
[2] D.M. Van Wie, D.G. Drewry Jr., D.E. King, C.M. Hudson, The hypersonic environment: Required operating conditions and design challenges, J. Mater. Sci. 39 (2004) 5915–5924.
[3] D.M. Hulbert, D. Jiang, D.V. Dudina, A.K. Mukherjee, The synthesis and consolidation of hard materials by spark plasma sintering, Int. J. Refract. Met. Hard Mater. 27 (2009) 367–375.

[4] F. Monteverde, A. Bellosi, Oxidation of $ZrB_2$-based ceramics in dry air, J. Electrochem. Soc. 150 (2003) B552–B559.
[5] W.G. Fahrenholtz, G.E. Hilmas, A.L. Chamberlain, J.W. Zimmermann, Processing and characterization of $ZrB_2$-based ultra-high temperature monolithic and fibrous monolithic ceramics, J. Mater. Sci. 39 (2004) 5951–5957.
[6] F. Monteverde, C. Melandri, S. Guicciardi, Microstructure and mechanical properties of an $HfB_2$ + 30 vol.% SiC composite consolidated by spark plasma sintering, Mater. Chem. Phys. 100 (2006) 513–519.
[7] R. Licheri, R. Orrù, C. Musa, A.M. Locci, G. Cao, Consolidation via spark plasma sintering of $HfB_2$/SiC and $HfB_2$/HfC/SiC composite powders obtained by self-propagating high-temperature synthesis, J. Alloys Compd. 478 (2009) 572–578.
[8] C.M. Carney, T.-I. Mah, Current isolation in spark plasma sintering of conductive and nonconductive ceramics, J. Am. Ceram. Soc. 91 (10) (2008) 3448–3450.
[9] C.M. Carney, Oxidation resistance of hafnium diboride–silicon carbide from 1400 to 2000 °C, J. Mater. Sci. 44 (20) (2009) 5673–5681.
[10] D. Sciti, L. Silvestroni, M. Nygren, Spark plasma sintering of Zr- and Hf-borides with decreasing amounts of $MoSi_2$ as sintering aid, J. Eur. Ceram. Soc. 28 (2008) 1287–1296.
[11] R. Licheri, R. Orrù, C. Musa, G. Cao, Combination of SHS and SPS techniques for fabrication of fully dense $ZrB_2$–ZrC–SiC composites, Mater. Lett. 62 (2008) 432–435.
[12] U. Anselmi-Tamburini, Y. Kodera, M. Gasch, C. Unuvar, Z.A. Munir, M. Ohyanagi, S.M. Johnson, Synthesis and characterization of dense ultra-high temperature thermal protection materials produced by field activation through spark plasma sintering (SPS): I. Hafnium diboride, J. Mater. Sci. 41 (10) (2006) 3097–3104.
[13] R. Caruso, N. Mamana, E. Benavidez, Densification kinetics of $ZrO_2$-based ceramics using a master sintering curve, J. Alloys Compd. 495 (2010) 570–573.
[14] M. Mazaheri, A. Simchi, M. Dourandish, F. Golestani-Fard, Master sintering curves of a nanoscale 3Y-TZP powder compacts, Ceram. Int. 35 (2009) 547–554.
[15] D.C. Blaine, J.D. Gurosik, S.J. Park, R.M. German, D.F. Heaney, Metall, Mater. Trans. A: Phys. Metall. Mater. Sci. 37A (2006) 715–720.
[16] D. Li, S. Chen, W. Shao, X. Ge, Y. Zhang, S. Zhang, Densification evolution of $TiO_2$ ceramics during sintering based on the master sintering curve theory, Mater. Lett. 62 (2007) 849–851.
[17] K.G. Ewsuk, D.T. Ellerby, C.B. DiAntonio, Analysis of nanocrystalline and microcrystalline ZnO sintering using master sintering curves, J. Am. Ceram. Soc. 89 (6) (2006) 2003–2009.
[18] M. Bothara, S.V. Atre, S.J. Park, R.M. German, T.S. Sudarshan, Sintering behavior of nanocrystalline silicon carbide using a plasma pressure compaction system: master sintering curve analysis, Metall. Mater. Trans. A 41 (12) (2010) 3252–3261.
[19] M. Gasch, D. Ellerby, E. Irby, S. Beckman, M. Gusman, S. Johnson, Processing and properties and arc jet oxidation of hafnium diboride/silicon carbide ultra high temperature ceramics, J. Mater. Sci. 39 (19) (2004) 5925–5937.
[20] E. Opila, S. Levine, J. Lorincz, Oxidation of $ZrB_2$- and $HfB_2$-based ultra-high temperature ceramics: effect of Ta additions, Mater. Sci. 39 (19) (2004) 5969–5977.
[21] J. Bull, M.J. White, L. Kaufman, US Patent No. 5750450 (1998).
[22] F. Monteverde, Progress in the fabrication of ultra-high-temperature ceramics: in situ synthesis, microstructure and properties of a reactive hot-pressed $HfB_2$–SiC composite, Compos. Sci. Technol. 65 (11–12) (2005) 1869–1879.
[23] F. Monteverde, A. Bellosi, Efficacy of HfN as sintering aid in the manufacture of ultrahigh-temperature metal diborides–matrix ceramics, J. Mater. Res. 19 (12) (2004) 3576–3585.